

# Simulation of Grid-Connected Photovoltaic System

Jingzhe Song (js4153)

**Abstract**—This paper simulates a grid-connected photovoltaic system in MATLAB/Simulink. The system consists of a PV cell, a DC/DC boost converter, and a DC/AC inverter. The paper starts with engineering approximation of photovoltaic cell. The PV cell model is easy, accurate, and takes external temperature and solar radiation into consideration. It also proposes a maximum power point tracking (MPPT) algorithm. The algorithm incorporated in a DC/DC converter is used to track the maximum power of PV cell. Finally, the DC/AC inverter is used to regulate the output voltage of DC/DC converter and connects the PV cell to the grid. Simulation results show that the model can effectively realize the actual physical characteristics of a grid-connected PV system.

**Index Terms**—photovoltaic system, MPPT, grid-connected

## I. INTRODUCTION

Among a variety of renewable energy sources, solar energy is predicted to become the largest contributors to world energy for its clean and no supply limitations characteristic. Over the past decade, PV technology has shown the potential by robust and continuous growth even during times of financial crisis. At the end of 2009, the world's PV cumulative installed capacity was approaching 23 GW. One year later it was 40 GW. In 2011, more than 69 GW are installed globally and could produce 85 TWh of electricity every year. This energy volume is sufficient to cover the annual power supply needs of over 20 million households. Figure 1 shows the evolution of global cumulative installed capacity 2000-2011 [1].

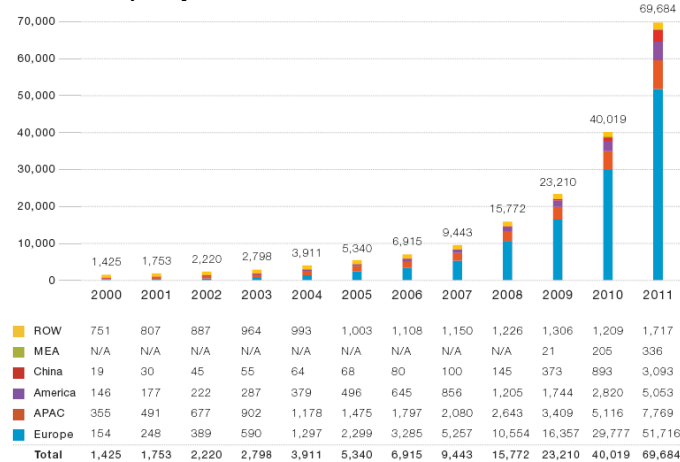


Figure 1. Evolution of global cumulative installed capacity 2000-2011

The key technology of a PV system includes PV cell modeling, maximum power point tracking (MPPT) algorithm, DC/DC converter and grid-connected DC/AC inverter.

This paper is organized as follows. In Section II, we take engineering approximation to simplify the ideal PV cell model, modify the model with consideration of changing temperature and solar radiation. In Section III, after comparing various MPPT control algorithms, we proposed an adjusted P&O method and simulate it in MATLAB/Simulink. Section IV

focuses on explaining the reason for choosing boost converter as the DC/DC converter and its operating principle. Section V explains the DC/AC inverter first, then brings out the whole PV system simulation model, and discussed the simulation result.

## II. MODELING OF PHOTOVOLTAIC CELL

### A. Ideal PV Cell

Photovoltaic (PV) cell is a semiconductor device that absorbs and converts the energy of light into electricity by photovoltaic effect. Figure 2 shows the equivalent circuit of the ideal PV cell.

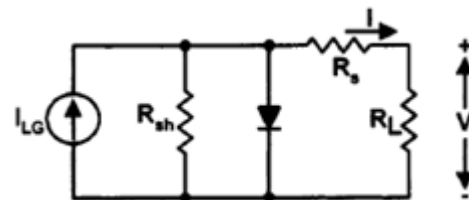


Figure 2. Equivalent circuit of ideal PV cell

The corresponding I-V characteristic of the photovoltaic cell is as below [2].

$$I = I_{LG} - I_d - I_{R_{sh}} = I_{LG} - I_{os} \left\{ \exp \left[ \frac{q}{AKT} (V + IR_s) \right] - 1 \right\} - \frac{V + IR_s}{R_{sh}} \quad (1)$$

$$\text{where, } I_{os} = I_{or} \left[ \frac{T}{T_r} \right]^3 \exp \left[ \frac{qE_{GO}}{Bk} \left( \frac{1}{T_r} - \frac{1}{T} \right) \right] \quad (2)$$

$$I_{LG} = [I_{SCR} + K_l(T - 298)] \frac{S}{1000} \quad (3)$$

I: Cell output current. (A)

V: Cell output voltage. (V)

$I_{LG}$ : Photon current. (A)

$I_{os}$ : PV cell's reverse saturation current. (A)

T: PV cell operating temperature. (K)

k: Boltzmann's constant. ( $1.38 \cdot 10^{-23}$  J/K)

q: Electron charge. ( $1.6 \cdot 10^{-19}$  C)

$K_l$ : Temperature coefficient of the short-circuit current. (A/K)

S: Operating solar radiation. ( $W/m^2$ )

$I_{SCR}$ : Short circuit current at STC. (A)

$E_{GO}$ : Bandgap energy of the semiconductor. (J)

A, B: Ideality constant, between 1 and 2.

$T_r$ : PV cell absolute temperature at STC (Standard Test Condition). (301.18 K)

$I_{or}$ : PV cell's reverse saturation current at temperature  $T_r$ . (A)

$R_{sh}$ : PV cell intrinsic parallel resistance. ( $\Omega$ )

$R_s$ : PV cell intrinsic series resistance. ( $\Omega$ )

### B. Engineering PV Cell Model

In the ideal PV Cell model,  $I_{LG}$ ,  $I_{os}$ ,  $R_{sh}$ , and  $R_s$  are related to cells temperature and radiation intensity, and are not easy to be determined. This makes the engineering application very difficult. Manufacturers of PV arrays provide only a few experimental technical parameters such as open-circuit voltage

$V_{OC}$ , short-circuit current  $I_{SC}$ , the maximum power point voltage  $V_m$ , the maximum power point current  $I_m$ , and the maximum power point power  $P_m$

Simplify the ideal PV model to match with the parameters provided by industry as below.

Normally,  $R_{sh}$  is between  $100\Omega$  and  $10000\Omega$ , so  $\frac{V+IR_s}{R_{sh}}$  can be ignored compared with Photon current  $I_{LG}$ .  $R_s$  is less than  $1\Omega$ , so  $I_{LG} = I_{SC}$ .

Under open-circuit state,  $I=0$ ,  $V = V_{OC}$ :

$$I = I_{SC} \left\{ 1 - C_1 \left[ \exp\left(\frac{V}{C_2 V_{OC}}\right) - 1 \right] \right\} \quad (4)$$

At the maximum power point, when  $V = V_m$ ,  $I = I_m$ :

$$I_m = I_{SC} \left\{ 1 - C_1 \left[ \exp\left(\frac{V_m}{C_2 V_{OC}}\right) - 1 \right] \right\} \quad (5)$$

Under normal temperature,

$$\exp\left(\frac{V_m}{C_2 V_{OC}}\right) \gg 1, \quad C_1 = \left(1 - \frac{I_m}{I_{SC}}\right) \exp\left(\frac{-V_m}{C_2 V_{OC}}\right) \quad (6)$$

Under open-circuit state, when  $I=0$ ,  $V = V_{OC}$ , therefore,

$$0 = I_{SC} \left\{ 1 - \left(1 - \frac{I_m}{I_{SC}}\right) \exp\left(\frac{-V_m}{C_2 V_{OC}}\right) \left[ \exp\left(\frac{1}{C_2}\right) - 1 \right] \right\} \quad (7)$$

Under normal temperature,

$$\exp\left(\frac{1}{C_2}\right) \gg 1, \quad C_2 = \left(\frac{V_m}{V_{OC}} - 1\right) / \ln\left(1 - \frac{I_m}{I_{SC}}\right) \quad (8)$$

Being seen, with common parameters like  $V_{OC}$ ,  $I_{SC}$ ,  $V_m$ ,  $I_m$ ,  $C_1$  and  $C_2$  can be calculated and the PV cell model can be created.

### C. Adjusting the Model

The above model is created under temperate  $25^\circ\text{C}$ ,  $1000\text{ W/m}^2$ . Considering variable ambient temperature and solar radiation, the model can be adjusted as below<sup>[3]</sup>.

$$T_c = T_a + t_c S \quad (9)$$

$$I = I_{SC} \left\{ 1 - C_1 \left[ \exp\left(\frac{V-DV}{C_2 V_{OC}}\right) - 1 \right] \right\} + DI \quad (10)$$

$$\text{where} \quad DI = \alpha \cdot \frac{S}{S_{ref}} \cdot DT + \left(\frac{S}{S_{ref}} - 1\right) \cdot I_{SC} \quad (11)$$

$$DV = -\beta \cdot DT - R_s \cdot DI \quad (12)$$

$$DT = T_c - T_{ref} \quad (13)$$

$I$  and  $V$  are the output current and voltage of the PV cell,  $I_{SC}$  is the short-circuit current,  $V_{OC}$  is the open-circuit voltage,  $S_{ref}$  and  $T_{ref}$  are the reference solar radiation and temperature,  $\alpha$  is the temperature coefficient of the short-circuit current,  $\beta$  is the temperature coefficient of the open-circuit voltage and  $R_s$  is the internal series resistance.

### D. Modeling and Simulation of PV cell in MATLAB/Simulink

Figure 3 and Figure 4 shows the simulation structure of the PV model and the packaged model in MATLAB/Simulink according to the improved PV cell model. The parameters used to define the PV cell are shown in Table I.

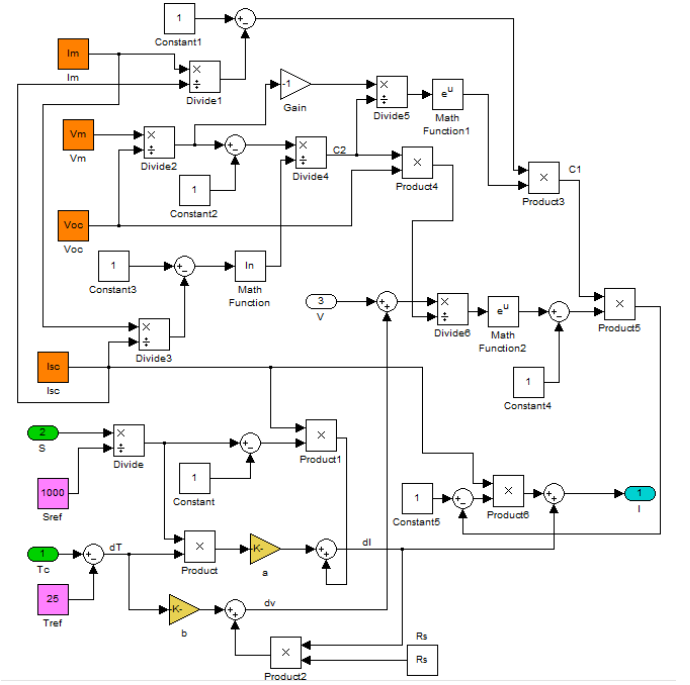


Figure 3. Simulation structure of PV model

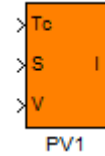


Figure 4. Packaged model of the PV cell

TABLE I. PARAMETERS OF THE PV CELL IN MATLAB/SIMULINK MODEL

Parameter	Variable	Value
Current at Maximum Power	$I_m$	4.95 A
Voltage at Maximum Power	$V_m$	35.2 V
Open Circuit Voltage	$V_{OC}$	44.2 V
Short Circuit Current	$I_{SC}$	5.2 A
Temperature Coefficient of Short Circuit Current	$a$	0.015 A/°K
Temperature Coefficient of Open Circuit Voltage	$b$	0.7V/°K
Internal Series Resistance	$R_s$	0.217Ω
Reference Solar Radiation	$S_{ref}$	1000 W/m <sup>2</sup>
Reference Temperature	$T_{ref}$	25 °C

The simulation result is shown in Figure 5 and Figure 6. Figure 5 shows the I-V characteristic curves of the PV cell. Figure 6 shows the P-V characteristic curves. The model curves exactly match with the experimental data at three remarkable points: short-circuit, open-circuit, and maximum power point. It can be seen that when the output voltage is less than a threshold value, the change of output current is very small with the changing of voltage. PV cell acts like a constant current source; when the output voltage exceeds a threshold value, the current declines sharply with increasing voltage. PV cell acts like a constant voltage source.

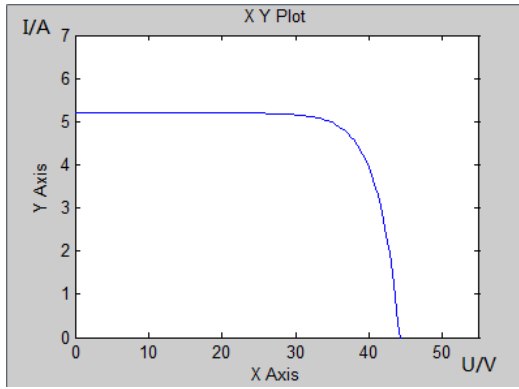


Figure 5. I-V characteristic curve of PV cell

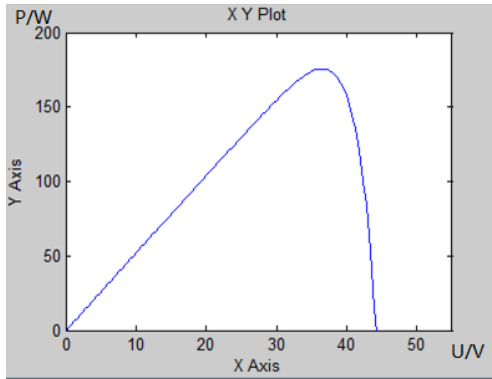


Figure 6. P-V characteristic curve of PV cell

### III. MPPT CONTROL ALGORITHM

On the I-V curve, there is a point where the PV cell generates the maximum power, this point always locates at the knee of the curve, and is called maximum power point (MPP). Since the output power of PV cell is related with many parameters such as solar radiation, temperature and load, the output characteristic is nonlinear. It is necessary for the PV system to work at the maximum power point under changing external environment to achieve best performance.

A MPPT is used for extracting the maximum power from the PV cell and transferring that power to the load<sup>[4]-[5]</sup>.

#### A. Comparison of Various MPPT algorithms

Various maximum power point tracking (MPPT) algorithms have been developed<sup>[6]-[7]</sup>. These algorithms differ from each other in terms of complexity, cost, and number of sensors used. Commonly used MPPT algorithms are listed as below.

1) *Perturb and Observe (P&O)*<sup>[8]-[9]</sup> and *Hill Climbing (HC)*<sup>[10]-[11]</sup> methods. The P&O method perturbs the operating voltage of PV cell, while the Hill Climbing method perturbs the duty ratio of power converter. These methods are easy to implement, but are not accurate and rapid enough since the effects of temperature and solar radiation has not been considered.

2) *Incremental Conductance (IC) method*<sup>[12]-[14]</sup>. This method uses the fact that the slope of the P-V curve is positive on the left of MPP and negative on the right of MPP,

It is an accurate and rapid method but is complex and put great requirements on the hardware

3) *Fractional Open Circuit Voltage method*<sup>[15]-[16]</sup> and *Fractional Short Circuit Current method*<sup>[17]-[19]</sup>. For the former method, the MPP voltage with respect to  $V_{OC}$  is monitored. For the latter method, the MPP current with respect to  $I_{SC}$  is monitored. These methods have low efficiency and their accuracy cannot be guaranteed under varying weather conditions, due to the approximation of a constant ratio.

#### B. Proposed MPPT Algorithm

In this paper, we choose the Perturb and Observe (P&O) method for its simplicity, relatively accuracy and rapid response. Figure 7 shows the flowchart of P&O method. By comparing PV cell output power of each control cycle before and after the perturbation, the new perturbation direction can be determined. If the output power is increasing, the previous voltage perturbation direction will be followed in the new cycle. Otherwise, the voltage perturbation direction will change. By this method, the operating point of PV cell can get closer to the maximum power point and finally reach a steady state.

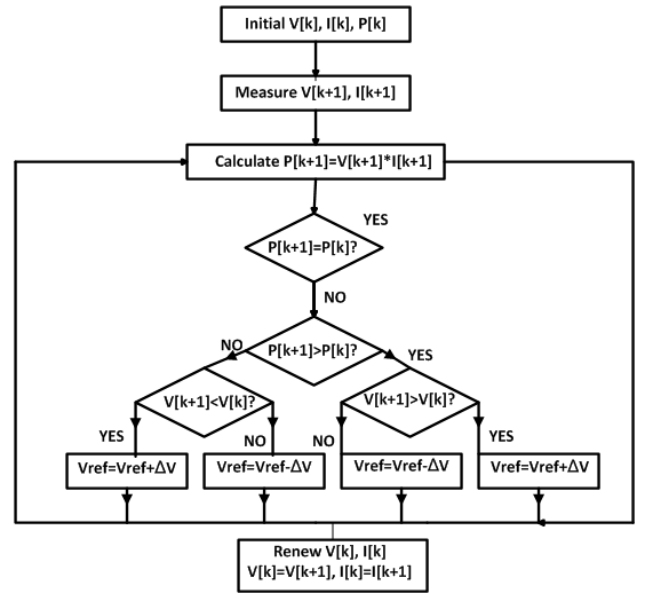


Figure 7. Flowchart of P&O Method

#### C. MPPT Algorithm Simulation in MATLAB/Simulink

The simulation model for P&O MPPT algorithm is shown in Figure 8. By comparing previous and current output power, new perturbation direction can be decided. If  $\Delta P * \Delta V > 0$ , the operating voltage should increase; while  $\Delta P * \Delta V < 0$ , the operating voltage should decrease. The operating voltage change is done by adjusting a step size  $\Delta D$  to the duty cycle  $D$  of a DC-DC converter. (The DC-DC converter will be introduced in Chapter IV).

This model has two parameters, the step size  $\Delta D$  and the time between iterations. The smaller the P&O step size, the more accuracy the result, and the longer the simulation time.

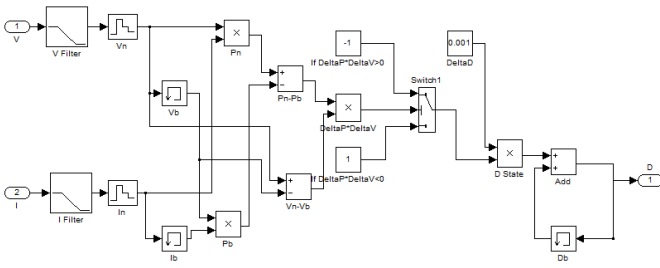


Figure 8. Simulation Model for P&O MPPT algorithm

#### IV. DC/DC CONVERTER

A DC/DC converter serves the purpose of transferring maximum power from the solar PV cell to the load. A DC/DC converter acts as an interface between the load and the PV cell. By changing the duty cycle, the load impedance is varied and matched at the point of the peak power with the source, so as to transfer the maximum power<sup>[20]</sup>.

There are Four basic topologies for DC/DC converter: Buck, Boost, Buck-Boost and Cuk.

##### A. Reason for Choosing Boost Converter

This paper chose the classical boost converter to implement the MPPT algorithm for the following reasons.

- 1) For Boost Converter, the output voltage is always higher than the input PV cell voltage, which is convenient for the PV cell to be connected to the grid later.
- 2) The topology for Boost Converter is simple, easy to implement, and has high efficiency.
- 3) The Boost Converter is easy to be controlled to minimize fluctuation and increase tracing accuracy.

##### B. Operating Principle of Boost Converter

Figure 9 shows the topology of Boost converter. For this converter, power flow is controlled by means of the on/off duty cycle of the switching transistor.

When the switch is On for  $t_{on}$  seconds, current flows through the inductor in clockwise, and energy  $V_i I_1 t_{on}$  is stored in the inductor.

When the switch is Off for  $t_{off}$  seconds, current will be reduced for increasing impedance. The only path of the inductor current is through diode D to the capacitor C and load R. The polarity of inductor will change. And the energy accumulated in the inductor during the On-State will be released,  $(V_c - V_i) I_1 t_{off}$ .

$$V_i I_1 t_{on} = (V_c - V_i) I_1 t_{off} \quad (14)$$

we have

$$V_c = \frac{t_{off}}{t_{on} + t_{off}} V_i = \frac{T}{t_{off}} V_i = \frac{1}{1-D} V_i \quad (15)$$

where D is the duty cycle. It represents the fraction of the commutation period T during which the switch is On.

Since  $\frac{T}{t_{off}} \geq 1$ , the output voltage is always higher than the source voltage.

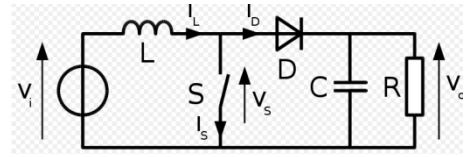


Figure 9. Topology of Boost Converter

##### C. Simulation of DC/DC Converter with MPPT algorithm in MATLAB/Simulink

A PWM boost converter with the following parameters is used for maximum power point tracking (Table II). The simulation model for DC/DC converter is shown in Figure 10.

TABLE II PARAMETERS OF THE DC/DC CONVERTER

Parameter	Value
Inductor L	0.01 H
Capacitor C1	$2 \times 10^{-3}$ F
Capacitor C	$2 \times 10^{-3}$ F
Resistor R	500Ω

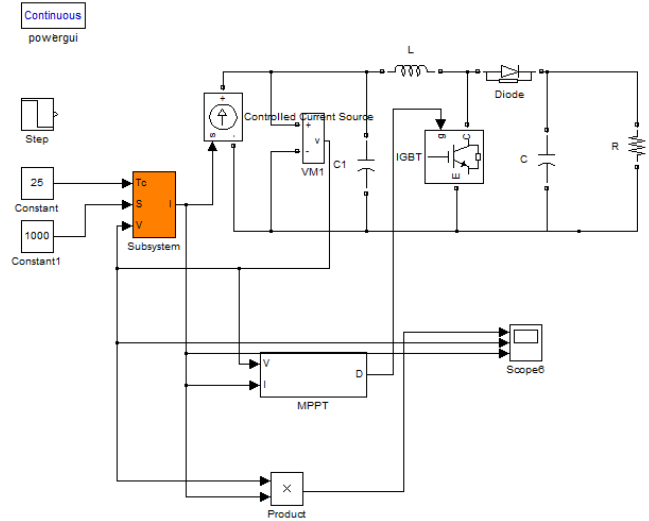


Figure 10. Simulation Model for DC/DC converter

1) When the temperature and solar radiation keeps unchanged,  $T=25^\circ\text{C}$ ,  $S=1000\text{ W/m}^2$ . The simulation result is shown in Figure 11. It can be seen from the figure that the system reaches the maximum power point at time  $t=0.2\text{ s}$ . Time  $t=0$  to  $t=0.05\text{ s}$  is a period for the system to initial its state, at time  $t=0.05\text{ s}$ , the PV cell has output voltage, but its current and output power is zero. From time  $t=0.05\text{ s}$  to  $t=0.2\text{ s}$ , the simulation waveform of MPPT control based on P&O method has overshoot, after  $t=0.2\text{ s}$ , the waveform shakes up and down regularly. This is due to the continuous comparison between each control cycle before and after the perturbation in the operation of the P & O method.

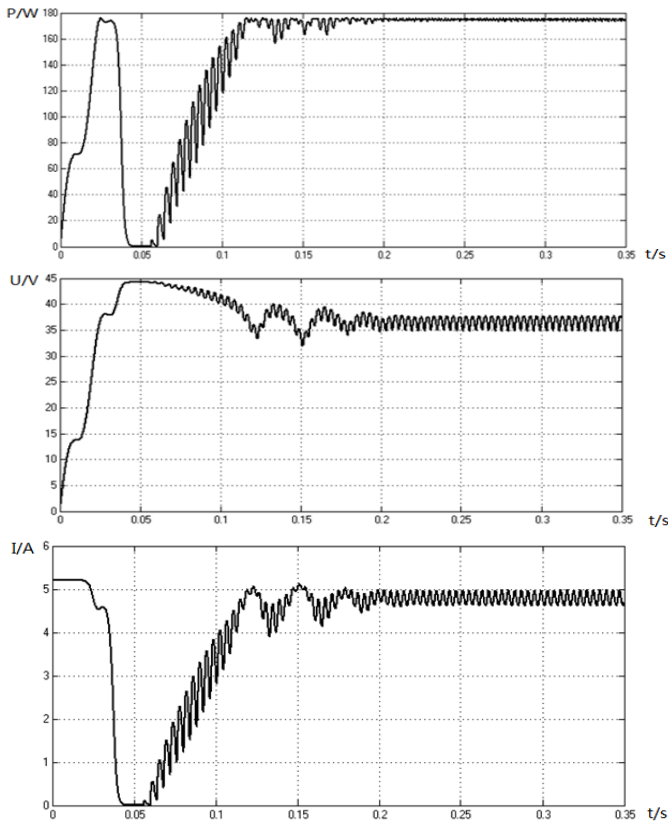


Figure 11. Simulation Results for MPPT when Temperature and Solar Radiation Keeps Unchanged,  $T=25^{\circ}\text{C}$ ,  $S=1000\text{ W/m}^2$ .

2) When the environment temperature keeps unchanged ( $25^{\circ}\text{C}$ ), and the solar radiation changes from  $1000\text{ W/m}^2$  to  $400\text{ W/m}^2$  at time  $t=0.3\text{s}$ . The simulation result is shown in figure 12. It is obvious that at time  $t=0.3\text{s}$  the output power decreases, the output voltage increases and the output current increases. After time  $t=0.5\text{s}$  the waveform shakes up and down regularly. This model can work effectively when solar radiation varies sharply.

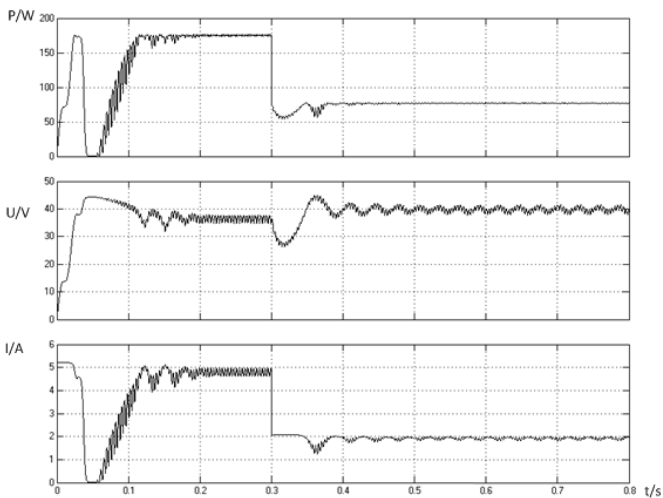


Figure 12. Simulation Results for MPPT when Temperature keeps unchanged ( $25^{\circ}\text{C}$ ), solar radiation changes from  $1000\text{ W/m}^2$  to  $400\text{ W/m}^2$

3) When the solar radiation keeps unchanged at  $1000\text{ W/m}^2$ , the environment temperature changes at  $t=0.5\text{s}$  from  $85^{\circ}\text{C}$  to  $25^{\circ}\text{C}$ . The simulation result is shown in Figure 13. It is obvious that at time  $t=0.5\text{s}$  the output power, voltage and current increase. After time  $t=0.5\text{s}$  the waveform shakes up and down regularly. This model can work effectively when external temperature varies sharply.

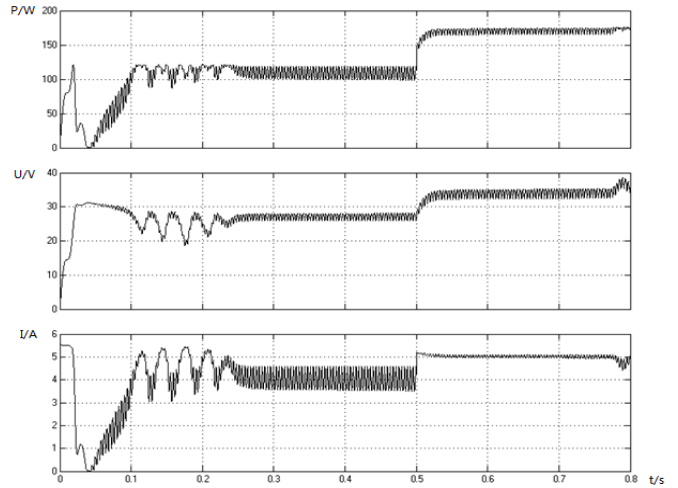


Figure 13. Simulation Results for MPPT When Solar Radiation Keeps Unchanged at  $1000\text{ W/m}^2$ , Temperature Changes at  $t=0.5\text{s}$  from  $85^{\circ}\text{C}$  to  $25^{\circ}\text{C}$

## V. DC/AC INVERTER

In this paper, the DC/AC Inverter is used to regulate the output voltage of DC/DC converter and connects the PV cell with DC/DC converter to the grid. The output voltage is required to be sinusoidal and in phase with the grid voltage. Figure 14 shows the whole PV grid-connected system. The DC/AC inverter is controlled by current-mode control. The reference current  $i^*$  is sent to compare with the DC/AC output current. The compared result is sent to a discrete PI controller to generate signals for a PWM generator. The PWM signal can be used to control switches of DC/AC inverter. The frequency of PWM waveform is set as  $5\text{ kHz}$ , which can reduce the switching noise, simplify the system design and improve the dynamic performance. In the PI controller,  $T=5 \times 10^{-7}$ ,  $K_p=6$ ,  $K_i=256$ . The AC Voltage Source represents grid voltage, Peak amplitude= $155.5\text{ V}$ , phase= $0$ , frequency= $60\text{ Hz}$ . In the LR filter,  $L_1=10\text{ mH}$ ,  $R=0.01\Omega$ .

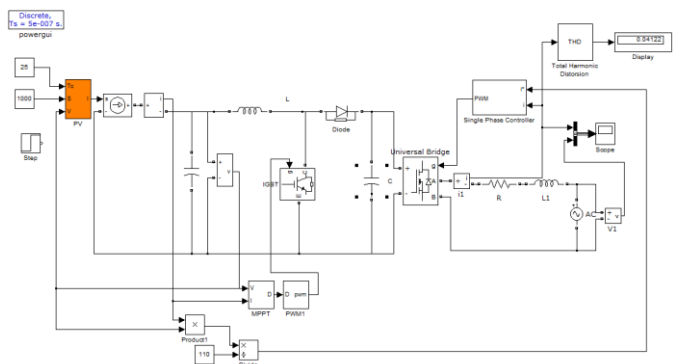


Figure 14. Whole PV Grid-Connected System

The structure of single phase controller is shown in Figure 15.

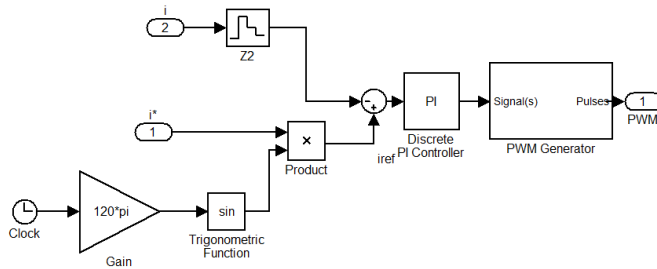


Figure 15. Structure of Single Phase Controller

1) When the temperature and solar radiation keeps unchanged,  $T=25\text{ }^\circ\text{C}$ ,  $S=1000\text{ W/m}^2$ . The simulation result is in Figure 16. At time  $t=0.05\text{ s}$ , the output current of the DC/AC inverter is almost sinusoidal and in phase with the grid voltage, the THD% of the DC/AC inverter's current is 4.122%, which satisfy the THD% requirements in standard UL1747 [20].

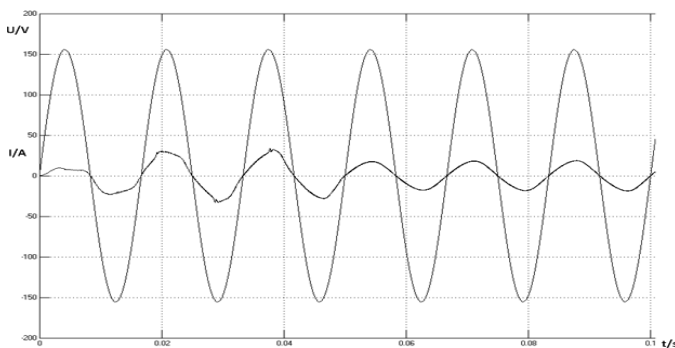


Figure 16. Simulation Results When Temperature and Solar Radiation Keeps Unchanged,  $T=25\text{ }^\circ\text{C}$ ,  $S=1000\text{ W/m}^2$ .

2) When the environment temperature keeps unchanged ( $25\text{ }^\circ\text{C}$ ), and the solar radiation changes from  $400\text{ W/m}^2$  to  $1000\text{ W/m}^2$  at time  $t=0.05\text{ s}$ . The result is shown in Figure 17. The output current increases at time  $t=0.05\text{ s}$ . After a short transition period, at time  $t=0.083\text{ s}$ , the output current of the DC/AC inverter is almost sinusoidal and in phase with the grid voltage again. The THD% of the DC/AC inverter's current is 3.147%, which satisfy the THD% requirements in standard UL1747 [20].

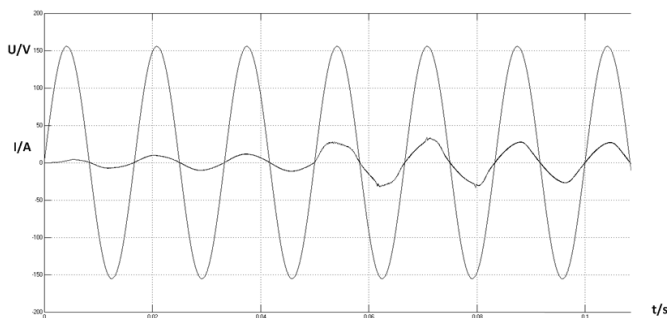


Figure 17. Simulation Results When Temperature keeps unchanged ( $25\text{ }^\circ\text{C}$ ), solar radiation changes from  $400\text{ W/m}^2$  to  $1000\text{ W/m}^2$

3) When the solar radiation keeps unchanged at  $1000\text{ W/m}^2$ , the environment temperature changes at  $t=0.1\text{ s}$ , from  $25\text{ }^\circ\text{C}$  to  $85\text{ }^\circ\text{C}$ . The result is shown in Figure 18. (In this part, the AC voltage source has been timed 0.3 to make the current change more obvious.) The output current decreases at time  $t=0.1\text{ s}$ , when the temperature from  $25\text{ }^\circ\text{C}$  to  $85\text{ }^\circ\text{C}$ . After a short transition period, the output current of the DC/AC inverter is almost sinusoidal and in phase with the grid voltage again. The THD% of the DC/AC inverter's current is 4.185%, which satisfy the THD% requirements in standard UL1747 [20].

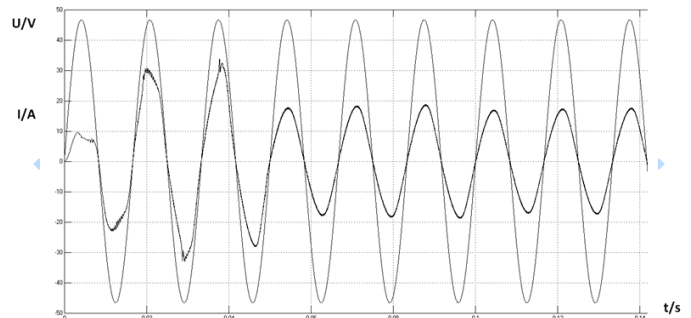


Figure 18. Simulation Results When Solar Radiation Keeps Unchanged at  $1000\text{ W/m}^2$ , Temperature Changes at  $t=0.1\text{ s}$  from  $25\text{ }^\circ\text{C}$  to  $85\text{ }^\circ\text{C}$

## CONCLUSION

In this paper, a modified engineering model for photovoltaic cell is proposed. This model can work well under sudden change of environment temperature or solar radiation. The maximum power of the PV cell is tracked with an adjusted P&O MPPT algorithm based on Boost DC/DC converter. A DC/AC inverter has been used to connect the PV cell to the grid and regulate the output voltage of DC/DC converter. The whole photovoltaic grid-connected system is simulated in MATLAB/Simulink. Special situations such as sudden change of temperature and solar radiation have been simulated and analyzed.

## REFERENCES

- [1] Global market outlook for photovoltaic until 2016, EPIA, 2012
- [2] H. S. Rauschenbach, *Solar Cell Array Design Handbook*. NewYork: Van Nostrand Reinhold, 1980.
- [3] Su Jianhui; Yu Shijie; Zhao Wei; Wu Minda; Shen Yuliang; He Huiruo. Investigation on Engineering Analytical Model of Silicon Solar Cells [J]. *Acta Energaiae Solaris Sinica*, 2001, 6(22): 439-412.
- [4] M.E.Ahmad and S.Mekhilef, "Design and Implementation of a Multi Level Three-Phase Inverter with Less Switches and Low Output Voltage Distortion," *Journal of Power Electronics*, vol. 9, pp. 594-604, 2009.
- [5] S. Chin, J. Gadson, and K. Nordstrom, "Maximum Power Point Tracker," Tufts University Department of Electrical Engineering and Computer Science, 2003, pp. 1-66.
- [6] T. ESRAM and P. L. Chapman, "Comparison of Photovoltaic Array Maximum Power Point Tracking Techniques," *IEEE Trans. on Energy Converters.*, vol. 22, no. 2, pp. 439 - 449, Jun. 2007
- [7] G. M. S. Azevedo, M. C. Cavalcanti, K. C. Oliveira, F. A. S. Neves, and Z. D. Lins, "Comparative Evaluation of Maximum Power Point Tracking Methods for Photovoltaic Systems," *Journal of Solar Energy Engineering*, vol. 131, no. 3, p. 31006, Aug. 2009.
- [8] J. J. Nedumgatt, K. B. Jayakrishnan, S. Umashankar, D. Vijayakumar, and D. P. Kothari, "Perturb and Observe MPPT Algorithm for Solar PV Systems-modeling and Simulation," in *Annual IEEE India Conference (INDICON)*, Dec. 2011, pp. 1 - 6.
- [9] L. Chun-xia and L. Li-qun, "An Improved Perturbation and Observation MPPT Method of Photovoltaic Generate System," in *4th IEEE*

- Conference on Industrial Electronics and Applications, ICIEA 2009., May. 2009, pp. 2966 - 2970.
- [10] W. Xiao and W. Dunford, "A Modified Adaptive Hill Climbing MPPT Method for Photovoltaic Power Systems," in IEEE 35th Annual Power Electronics Specialists Conference, PESC 04., vol. 3. IEEE, Jun. 2004, pp. 1957 - 1963.
- [11] F. Liu, Y. Kang, Y. Zhang, and S. Duan, "Comparison of P&O and Hill Climbing MPPT Methods for Grid-connected PV Converter," in 3rd IEEE Conference on Industrial Electronics and Applications, ICIEA 2008. IEEE, Jun. 2008, pp. 804 - 807.
- [12] K. H. Hussein, I. Muta, T. Hoshino, and M. Osakada, "Maximum Photovoltaic Power Tracking: An Algorithm for Rapidly Changing Atmospheric Conditions," IEE Proceedings - Generation, Transmission and Distribution, vol. 142, no. 1, pp. 59 - 64, Jan. 1995.
- [13] K. Irisawa, T. Saito, I. Takano, and Y. Sawada, "Maximum Power Point Tracking Control of Photovoltaic Generation System Under Non-uniform Isolation by Means of Monitoring Cells," in Conference Record of the Twenty-Eighth IEEE Photovoltaic Specialists Conference, 2000. IEEE, Sep. 2000, pp. 1707 - 1710.
- [14] Y. H. Ji, D. Y. Jung, J. G. Kim, J. H. Kim, T. W. Lee, and C. Y. Won, "A Real Maximum Power Point Tracking Method for Mismatching Compensation in PV Array under Partially Shaded Conditions," IEEE Trans. on Power Electronics., vol. 26, no. 4, pp. 1001 - 1009, Apr. 2011.
- [15] A. F. Murtaza, H. A. Sher, M. Chiaberge, D. Boero, M. D. Giuseppe, and K. E. Addoweesh, "A novel hybrid mppt technique for solar pv applications using perturb amp; observe and fractional open circuit voltage techniques," in 15th International Symposium MECHATRONIKA, 2012, Dec. 2012, pp. 1-8.
- [16] J. Ahmad, "A fractional open circuit voltage based maximum power point tracker for photovoltaic arrays," in 2nd International Conference on Software Technology and Engineering (ICSTE) 2010, vol. 1, Oct. 2010, pp. V1-247 -V1-250.
- [17] M. A. S. Masoum, H. Dehbonei, and E. F. Fuchs, "Theoretical and Experimental Analyses of Photovoltaic Systems with Voltage and Current-based Maximum Power-Point Tracking," IEEE Trans. on Energy Converters., vol. 17, no. 4, pp. 514 - 522, Dec. 2002.
- [18] S. Yuvarajan and S. Xu, "Photo-voltaic Power Converter with a Simple Maximum-Power-Point-Tracker," in Proceedings of the 2003 International Symposium on Circuits and Systems, ISCAS' 03., vol. 3. IEEE, May. 2003, pp. III-399- III-402.
- [19] D. P. Quoc, Q. N. Nhat, N. T. D. Vu, A. N. Bao, H. H. Lee et al., "The New Combined Maximum Power Point Tracking Algorithm using Fractional Estimation in Photovoltaic Systems," in IEEE Ninth International Conference on Power Electronics and Drive Systems (PEDS), 2011. IEEE, Dec. 2011, pp. 919 - 923.
- [20] UL1741, Inverter, Converter, and Controllers for Use in Independent Power System.